



RESEARCH PAPER

# The sequence and thresholds of leaf hydraulic traits underlying grapevine varietal differences in drought tolerance

Silvina Dayer<sup>1,\*</sup>, José Carlos Herrera<sup>2</sup>, Zhanwu Dai<sup>3</sup>, Régis Burllett<sup>4</sup>, Laurent J. Lamarque<sup>4</sup>, Sylvain Delzon<sup>4</sup>, Giovanni Bortolami<sup>5</sup>, Hervé Cochard<sup>6</sup> and Gregory A. Gambetta<sup>1</sup>

<sup>1</sup> EGFV, Bordeaux-Sciences Agro, INRA, Université de Bordeaux, ISVV, 210 Chemin de Leysotte 33882 Villenave d'Ornon, France

<sup>2</sup> Institute of Viticulture and Pomology, University of Natural Resources and Life Sciences (BOKU), 3430 Tulln, Austria

<sup>3</sup> Beijing Key Laboratory of Grape Science and Enology and Key Laboratory of Plant Resources, Institute of Botany, the Chinese Academy of Sciences, Beijing, 100093, China

<sup>4</sup> Biodiversité Gènes et Communautés, Institut National de la Recherche Agronomique (INRA), Université Bordeaux, 33610 Cestas, France

<sup>5</sup> SAVE, INRA, BSA, ISVV, 33882 Villenave d'Ornon, France

<sup>6</sup> Université Clermont-Auvergne, INRA, PIAF, 63000 Clermont-Ferrand, France

\* Correspondence: [silvinadayer@gmail.com](mailto:silvinadayer@gmail.com)

Received 5 November 2019; Editorial decision 2 April 2020; Accepted 10 April 2020

Editor: Howard Griffiths, University of Cambridge, UK

## Abstract

Adapting agriculture to climate change is driving the need for the selection and breeding of drought-tolerant crops. The aim of this study was to identify key drought tolerance traits and determine the sequence of their water potential thresholds across three grapevine cultivars with contrasting water use behaviors, Grenache, Syrah, and Semillon. We quantified differences in water use between cultivars and combined this with the determination of other leaf-level traits (e.g. leaf turgor loss point,  $\pi_{TLP}$ ), leaf vulnerability to embolism ( $P_{50}$ ), and the hydraulic safety margin (HSM  $P_{50}$ ). Semillon exhibited the highest maximum transpiration ( $E_{max}$ ), and lowest sensitivity of canopy stomatal conductance ( $G_c$ ) to vapor pressure deficit (VPD), followed by Syrah and Grenache. Increasing  $E_{max}$  was correlated with more negative water potential at which stomata close ( $P_{gs90}$ ),  $\pi_{TLP}$ , and  $P_{50}$ , suggesting that increasing water use is associated with hydraulic traits allowing gas exchange under more negative water potentials. Nevertheless, all the cultivars closed their stomata prior to leaf embolism formation. Modeling simulations demonstrated that despite a narrower HSM, Grenache takes longer to reach thresholds of hydraulic failure due to its conservative water use. This study demonstrates that the relationships between leaf hydraulic traits are complex and interactive, stressing the importance of integrating multiple traits in characterizing drought tolerance.

**Keywords:** Drought, embolism, grapevine, stomata, transpiration, turgor loss point.

## Introduction

In the context of climate change, the identification of key traits responsible for drought-tolerant species/genotypes has become a major challenge in plant research. There has been a huge

emphasis placed on genetics and genomics, but both of these approaches rely upon accurate identification and phenotyping of the underlying physiological traits (Cattivelli *et al.*, 2008).

Most studies aimed at the identification of vulnerable/tolerant genotypes are based on only one or a few traits (Tardieu and Simmoneau, 1998; Schultz, 2003; Pou et al., 2012; Hopper et al., 2014) and are often constrained to moderate drought stress (i.e. a narrow range of water potentials; Gerzon et al., 2015; Coupel-Ledru et al., 2017). We know that the traits contributing to drought tolerance are complex, involving morphological, physiological, and hydraulic mechanisms (Hochberg et al., 2017a). New state-of-the-art phenotyping approaches, including mini-lysimeter platforms (Coupel-Ledru et al., 2016, 2017; Charrier et al., 2018), hold promise to more precisely phenotype these traits. However, different phenotyping approaches need to be integrated to assess multiple traits across a full range of drought stress (i.e. from moderate to severe) in order to more accurately predict the behavior of genotypes under diverse environmental conditions.

Plants react to drought stress via a series of physiological, cellular, and molecular responses that converge in stress tolerance, avoidance, and/or escape (Delzon, 2015). While growth cessation has been identified as the earliest response to drought, stomatal closure is probably the most widely studied (Chaves et al., 2010). Stomatal closure regulates plant water use and protects the xylem network from hydraulic failure (i.e. embolism) and branch dieback (Tyree and Sperry, 1989). Although there is a relationship between transpiration rate, leaf water potentials, and guard cell turgor (Brodribb et al., 2003), there is still controversy regarding whether stomatal closure occurs well before, at, or even after the onset of embolism (Bartlett et al., 2016). The leaf turgor loss point ( $\pi_{\text{TLP}}$ ) is defined as the water potential at which cells lose turgor (Brodribb et al., 2003; Bartlett et al., 2012) and has been considered a key physiological trait given its close association with stomatal closure and vulnerability to embolism (Brodribb et al., 2003; Bartlett et al., 2016; Martin-StPaul et al., 2017; Zhu et al., 2018). The  $\pi_{\text{TLP}}$  is estimated from the relationship between leaf water potential and leaf water volume known as the pressure–volume (p–v) curve and is related to other parameters correlated to drought tolerance such as the relative water content ( $\text{RWC}_{\text{TLP}}$ ), the osmotic potential at full hydration ( $\pi_0$ ), the elastic modulus of the cell wall ( $\epsilon$ ), and the tissue capacitance (C) (Bartlett et al., 2012).

There is a well-known link between xylem embolism and mortality across tree species (Delzon and Cochard, 2014), and significant progress has been made in determining critical hydraulic thresholds for a number of woody species providing quantitative, ‘measurable’ indexes of their capacity to tolerate drought (Brodribb et al., 2010; Urli et al., 2013; Hammond et al., 2019). Species vary in their vulnerability to embolism and are typically compared using the water potential inducing 50% loss of hydraulic conductance ( $P_{50}$ ) (Choat, 2013). Vulnerability may not be physiologically relevant under most non-extreme conditions where water status is modulated largely via stomatal regulation (Meinzer et al., 2009). For example, most recent studies have shown that the hydraulic safety margin (HSM), defined as the difference between the water potential at stomatal closure ( $P_{g90}$ ) and  $P_{50}$ , may be more relevant in explaining plant mortality under drought than  $P_{50}$  alone (Anderegg et al., 2016). Because the HSM integrates many important aspects of plant structure (e.g. anatomical features of the xylem and

the cuticle) and physiology (e.g. stomatal conductance), its value across species is variable and related to the environment (Anderegg et al., 2016). Additionally, other traits (e.g. osmotic adjustment, the capacitance of plant tissues, root system properties, etc.) could explain differences in xylem pressure changes and the rate at which critical thresholds for hydraulic failure are reached between plant species (Anderegg and Meinzer, 2015; Choat et al., 2018). The recent Sur\_Eau model developed by Martin-St. Paul et al. (2017) was successful in creating a framework for defining drought-induced mortality and could potentially be used to integrate multiple drought-related traits in predicting the time to hydraulic failure for different genotypes.

The objective of this study was to leverage multiple state-of-the-art phenotyping approaches to integrate a range of traits responsible for the drought response in three grapevine cultivars with contrasting water use behaviors, across the full range of water potentials leading to plant mortality. We hypothesized that the differences in drought behavior between cultivars involves multiple traits and is determined by the sequence and magnitude of the water potential thresholds for these traits. We quantified differences in the grapevine cultivars’ regulation of water use and linked these differences to leaf hydraulic traits such as  $\pi_{\text{TLP}}$  and  $P_{50}$ , and the leaf HSM. To do so, we characterized each cultivar’s dynamic water use by continuously monitoring whole-plant transpiration and stomatal regulation using a greenhouse mini-lysimeter platform. Each cultivar’s corresponding leaf turgor loss point and its related parameters such as osmotic potential, modulus of elasticity, and leaf capacitance were determined through the construction of p–v curves. The leaf vulnerability to embolism was quantified in intact plants using the non-invasive optical technique (Brodribb et al., 2016), allowing a comparison of HSMs between the cultivars. Finally, we used a soil–plant water transport model to explore the different associations between  $E_{\text{max}}$ ,  $P_{g90}$ , and  $P_{50}$  in determining the survival time until hydraulic failure during drought.

## Materials and methods

### Plant material

One-year-old plants of own rooted *Vitis vinifera* L. ‘Grenache’, ‘Syrah’, and ‘Semillon’ from the INRA nursery (Villenave d’Ornon, France) were planted in 7 liter pots containing 1 kg of gravel and 5.5 kg of commercial potting medium (70% horticultural substrate and 30% sand). Plants were grown outside under well-watered conditions for ~2 months before the experiment started. The plants were drip irrigated with nutritive solution [ $\text{NH}_4\text{H}_2\text{PO}_4$  0.1 mmol  $\text{l}^{-1}$ ;  $\text{NH}_4\text{NO}_3$  0.187 mmol  $\text{l}^{-1}$ ;  $\text{KNO}_3$  0.255 mmol  $\text{l}^{-1}$ ;  $\text{MgSO}_4$  0.025 mmol  $\text{l}^{-1}$ ; 0.002 mmol  $\text{l}^{-1}$  Fe, and oligo-elements (B, Zn, Mn, Cu, and Mo)] to avoid any deficiency during their development, and the surface of the pots were covered with a plastic bag to prevent water loss by soil evaporation.

### Mini-lysimeter phenotyping platform experiment

On 20 July, 15 plants from each cultivar were transferred to an automated mini-lysimeter greenhouse phenotyping platform where pots were continuously weighed on individual scales (CH15R11, OHAUS type CHAMP, Nänikon, Switzerland) and watered daily based on the plant weight loss by transpiration. The day before the experiment started, all the pots were irrigated up to their pot capacity weight and allowed

to drain overnight. A dry-down experiment was imposed on 10 vines per cultivar by stopping irrigation on two different dates: 16 August on a set of five plants ( $n=5$ ) per cultivar and 23 August on another set of five plants (each drying cycle lasted between 12 d and 15 d). A set of five well-watered vines per cultivar were kept as controls concomitantly with the water-stressed plants during each drying cycle. Air temperature, relative humidity, and radiation conditions were automatically monitored every 20 min at three different positions in the greenhouse. Air temperature was maintained approximately below 25 °C by the cooling system of the greenhouse to avoid any heat stress. The experimental design within the platform was completely randomized.

### Balance data analysis

The transpiration per leaf area ( $E$  in  $\text{mmol m}^{-2} \text{s}^{-1}$ ) was calculated as:

$$E = \Delta_w / \text{AL} / \text{MW}_w \quad (1)$$

where  $\Delta_w$  is the change in weight within the considered period ( $\text{g s}^{-1}$ ), AL is the leaf area ( $\text{m}^2$ ), and  $\text{MW}_w$  the molecular weight of water ( $18 \text{ g mol}^{-1}$ ).

The canopy stomatal conductance  $G_c$  ( $\text{mmol m}^{-2} \text{s}^{-1}$ ) was calculated using the simplification suggested by Monteith and Unsworth (1990):

$$G_c = K_G(T) \times E/D \quad (2)$$

Where  $K_G(T)$  is the conductance coefficient in  $\text{kPa m}^3 \text{kg}^{-1}$  (Ewers *et al.*, 2001) which accounts for temperature effects on the psychrometric constant, latent heat of vaporization, specific heat of air at constant pressure, and the density of air (Phillips and Oren 1998),  $E$  is the transpiration ( $\text{mmol m}^{-2} \text{s}^{-1}$ ), and  $D$  is the vapor pressure deficit (VPD;  $\text{kPa}$ ) calculated from the temperature and relative humidity data, as indicated in the infrared gas analyzer manual WALZ GFS-3000.

The  $G_c$  values obtained were filtered by light in order to always have saturating values of radiation [photosynthetic photon flux density (PPFD)  $>800 \mu\text{mol m}^{-2} \text{s}^{-1}$ ].

The water status of the plants during the experiment was monitored by measuring the pre-dawn leaf water potential ( $\psi_{\text{pd}}$ ) on 3–4 plants per cultivar and treatment. Measurements were performed in a basal fully expanded leaf prior any light exposure (between 05.00 h and 06.00 h) every 2–3 d using a Scholander pressure chamber (Precis 2000, Gradignan, France).

The leaf area was estimated through the relationship obtained between the leaf midrib length and the leaf area (measured with a leaf area meter Model LI-3000, LI-COR, Lincoln, NE, USA) for each cultivar using ~200 leaves per cultivar. The leaf midrib length was measured weekly on all the leaves of each plant, and the respective total leaf area per plant was then calculated using the equations obtained.

Additional measurements of stomatal conductance were taken in fully expanded, mature leaves (8th–10th node) from all the cultivars and treatments. The measurements were taken at 11.00 h during the 15 d of the experiment with a porometer (SC-1, Decagon Devices, WA, USA).

### Leaf turgor loss and minimum conductance

From the same set of plants, four plants per cultivar ( $n=4$ ) were selected to construct the  $p$ - $v$  curves by progressively drying leaves on a laboratory bench ('bench dry method'; Sack and Pasquet-Kok, 2011) and measuring the  $\psi_{\text{leaf}}$  and leaf mass at determined intervals. The plants were well watered to pot capacity the previous day and drained overnight. In the morning (09.00–09.30 h), one healthy mature leaf (8th–10th leaf from the shoot base) was cut at the base with a razor blade, sealed in a plastic bag (Whirl-Pak), and its leaf water potential ( $\psi_{\text{leaf}}$ ) was measured with a Scholander pressure chamber (Precis 2000). The leaf mass was immediately registered in an analytical balance and the leaf was placed on a bench at room temperature (23 °C) to let it dehydrate until the next  $\psi_{\text{leaf}}$  and mass measurements. The time elapsed between measurements attempted to capture intervals of  $\psi_{\text{leaf}}$  of 0.2–0.3 MPa until at least five points were obtained beyond the point at which zero turgor was attained.

The  $p$ - $v$  curves were constructed by plotting the inverse of leaf water potential ( $-1/\psi_{\text{leaf}}$ ) against the relative water content (RWC) which facilitated the determination of the turgor loss point as the point of transition between linear and non-linear portions (Supplementary Fig. S1 at JXB online; Tyree and Hammel, 1972). Leaf RWC was calculated as:  $\text{RWC} = (\text{FW} - \text{DW}) / (\text{turgid weight} - \text{DW}) \times 100$ . From the  $p$ - $v$  curves,  $\psi_{\text{leaf}}$  at the turgor loss point ( $\pi_{\text{TLP}}$ ), osmotic potential at full turgor ( $\pi_0$ ), and modulus of elasticity ( $\epsilon$ ) were calculated according to Bartlett *et al.* (2012). Leaf capacitance ( $C_{\text{leaf}}$ ) was calculated from the change in volume per change in water potential at full turgor ( $C_{\text{FT}}$ ), and below the turgor loss point ( $C_{\text{TLP}}$ ).

In the same set of plants used to produce the  $p$ - $v$  curves, minimum conductance (minimum water loss after stomatal closure) was determined in eight leaves from the three cultivars by using the 'mass loss of detached leaves' technique (Duursma *et al.*, 2019). The technique consists of measuring the leaf mass loss monitored over time as the leaf dries out. Leaves from well-watered plants were detached and suspended by their petiole (to allow the lamina to transpire from both sides) in a controlled chamber (Fitoclima 1200, Aralab, Portugal) set to a constant temperature of 25 °C and relative humidity of 45%. PPFD at the position of the samples was  $\sim 400 \pm 50 \mu\text{mol m}^{-2} \text{s}^{-1}$ . The mass loss of the leaves was recorded every 5–10 min for the first hour and then every 15–20 min as long as the leaves dehydrated with a 0.0001 g resolution balance (Sartorius LE5201 Expert, Goettingen, Germany). A relationship between leaf mass and time allowed us to determine that initial water loss rates are high and after some time a constant flow is achieved. The minimum conductance ( $g_{\text{min}}$ ) is calculated by using the measured VPD according to the equation  $E = g_{\text{min}} \times D/P$  where  $D$  is the VPD in  $\text{kPa}$  and  $P$  is the atmospheric pressure expressed in  $\text{mmol m}^{-2} \text{s}^{-1}$  (Duursma *et al.*, 2019). The minimum conductance determined by this technique was used as a proxy of the 'cuticular conductance' as it has been recently observed in eight species that both conductances are comparable (Schuster *et al.*, 2017).

### Non-invasive optical determination of leaf vulnerability

Leaf embolism formation and propagation were evaluated in four individuals per cultivar ( $n=4$ ) by monitoring changes in light transmission through the xylem (Brodribb *et al.*, 2016). Intact plants (well-watered) were placed in a room with controlled conditions at 26 °C and 50% relative humidity, and irrigation was cut off at the beginning of the scanning. For each plant, the abaxial side of an intact mature leaf (taken from the 8th–10th node), still attached to the parent vine, was fixed on a scanner (Perfection V800 Photo, EPSON, Suna, Japan) using a transparent glass and adhesive tape. The imaged area consisted of half of each leaf including the midrib, and the scanner magnification was set to give enough resolution of the midrib and at least eight major (second-order) veins. Brightness and contrast as well as leaf scanned area were adjusted to optimize visualization of embolisms and provide images not exceeding 9 Mbyte. Each leaf was automatically scanned every 5 min throughout plant dehydration using a computer automation software (AutoIt 3).

Simultaneous measurements of stem water potential ( $\psi_{\text{stem}}$ ) were made using psychrometers (ICT Internationale, Armidale, NSW, Australia) properly installed on the main stem adjacent to the scanned leaf. The  $\psi_{\text{stem}}$  values were automatically recorded every 30 min and the accuracy of the readings was confirmed by  $\psi_{\text{leaf}}$  measurements on basal leaves previously bagged with aluminum foil (2 h at least) using a Scholander pressure bomb (Precis 2000).

The stack of images captured at the end of the experiment comprised between 1800 and 2000 scans per leaf and they were analyzed using ImageJ software and following instructions from <http://www.opensourceov.org>. Briefly, total embolism was quantified by subtracting pixel differences between consecutive images (i.e. pixel values that did not change resulted in a value of zero). In these series, white pixels represented leaf embolism. Noise was removed using the ImageJ outlier removal, and pixel thresholding was used to extract embolism from any background noise remaining. The embolism area per image was calculated as the sum of non-zero pixels and expressed as cumulative embolisms, a percentage of total embolism area in the sequence.

Vulnerability curves corresponding to the percentage of embolized pixels (PEP) as a function of  $\psi_{\text{stem}}$  were fitted based on the following equation (Pammenter and Van der Willigen, 1998):

$$\text{PEP} = \frac{100}{1 + e^{(\text{slp}/25 \cdot (-P_{50}))}} \quad (3)$$

where  $P_{50}$  (MPa) is the  $\psi_{\text{stem}}$  value at which 50% of the xylem embolisms were observed and  $\text{slp}$  (%  $\text{MPa}^{-1}$ ) is the slope of the vulnerability curve at the inflexion point. The xylem pressure inducing the 12% ( $P_{12}$ ) and 88% ( $P_{88}$ ) of embolism loss of functionality were calculated as follows:  $P_{12} = 50/\text{slp} + P_{50}$  and  $P_{88} = -50/\text{slp} + P_{50}$ . One vulnerability curve was obtained per leaf per plant ( $n=4$  per cultivar).

Finally, to visualize the dynamics of embolism spread through the leaf, spatio-temporal color maps of embolism formation were created for some of the samples by coloring the embolism area in each sequence using a color scale of  $\psi_{\text{stem}}$  over time.

### Model simulations of hydraulic traits

A soil–plant water transport model (Sur\_Eau; Martin-StPaul et al., 2017) was used to determine the predicted survival time until hydraulic failure under drought for each cultivar. A detailed explanation of the model is given in Martin-StPaul et al. (2017). Briefly, the plant is described as a series of variable symplasmic and apoplasmic hydraulic conductances and capitals that determine water flows and water potential along the soil–plant–atmosphere continuum. The model computes the leaf transpiration, driven by leaf–air VPD, its regulation by stomatal closure, and thus the variation in soil water content. Beyond the point of stomatal closure, residual leaf transpiration is maintained, leading to plant dehydration and hydraulic failure under extreme water stress. Environmental conditions were either constant ( $T_{\text{air}}=25$  °C,  $\text{RH}_{\text{air}}=50\%$ ,  $\text{PAR}=400$   $\mu\text{mol m}^{-2} \text{s}^{-1}$ ) or variable during the day (night:  $T_{\text{air}}=20$  °C,  $\text{RH}_{\text{air}}=90\%$ ,  $\text{PAR}=0$   $\mu\text{mol m}^{-2} \text{s}^{-1}$ ; day as above). All plant parameters were identical for the three genotypes, except for the maximal stomatal conductance, the leaf osmotic potential at full turgor, the modulus of elasticity, the  $P_{50}$ , and the stomatal response curve to leaf water potential that were adjusted to actual values measured on each genotypes. The simulations were performed at a time step of 0.01 s and stopped when 99.99 loss of hydraulic conductivity (PLC) was reached in the leaf apoplasm, thus defining the time to hydraulic failure.

### Statistical analyses

Statistical analyses and fit were performed using R software (<http://www.R-project.org>) and GraphPad Prism version 7.00 for Windows (GraphPad Software, La Jolla, CA, USA).

To extrapolate water potentials obtained during the dry-down experiment at the lysimeter platform,  $\psi_{\text{PD}}$  was calculated from RWC using a Campbell (1974) equation modified by Van Genuchten (1980) (Charrier et al., 2018; Supplementary Fig. S2):

$$\psi_{\text{PD}} = a \times (\text{RWC})^b + \psi_e \quad (4)$$

where  $\psi_e$  is the soil water potential at the air entry point.

The soil RWC of each pot was calculated as  $\text{RWC} = (\text{actual weight} - \text{DW}) / (\text{saturated weight} - \text{DW})$ . The saturated weight corresponded to the total pot weight registered after watering the plants to pot (or field) capacity at the end of the afternoon and drained overnight. The actual weight corresponded to the weight registered by the balances during the dry-down experiment, and the dry weight corresponded to the weight of a pot after placing in an oven for 48 h at 60 °C. The weight of the soil substrate was obtained by subtracting the weight of the pot and draining gravel (which was standardized between pots).

Stomatal conductance ( $G_c$ ), depending on pre-dawn leaf water potential, was fit according to the following sigmoid function:

$$G_c = \frac{g_{sm}}{1 + e^{\text{slp} \cdot (-P_{g50})}} \quad (5)$$

where  $g_{sm}$  corresponds to maximal stomatal conductance at  $\psi=0$ ,  $\text{slp}$ , the sensitivity to decreasing water potential, and  $P_{g50}$  the water potential inducing 50% stomatal closure.

Linear regressions between  $G_c$  and VPD were calculated for each cultivar, and the slopes and intercepts were compared at  $P < 0.05$  using analysis of covariance (ANCOVA) in R. For non-linear regressions ( $G_c$  and  $E$  versus  $\psi_{\text{PD}}$ ), the Akaike information criterion (AICc) method was used to compare different fits.

Difference in  $P_{50}$ ,  $P_{12}$ ,  $P_{88}$ , and  $\text{slp}$ , and  $p-v$  results were tested with one-way ANOVA and post-hoc Tukey HSD test ( $< 0.05$ ). The HSM was calculated for each cultivar as the difference between the water potential at  $P_{Gc90}$  and the water potential at stem  $P_{50}$ .

## Results

### Water use under non-limiting water conditions

Under well-watered conditions, diurnal rates of transpiration ( $E$ ) in all plants increased from minimum values overnight to maximum rates ( $E_{\text{max}}$ ) at  $\sim 14$  h and were maintained for several hours (Fig. 1). Significant differences were observed in  $E_{\text{max}}$  between cultivars, with Semillon showing the highest rate, 2.1  $\text{mmol H}_2\text{O m}^{-2} \text{s}^{-1}$ , and Grenache the lowest, 1.4  $\text{mmol H}_2\text{O m}^{-2} \text{s}^{-1}$ . It is important to mention that the total leaf area was slightly lower in Semillon ( $\sim 17\%$  lower than both Syrah and Grenache); however, these differences did not result in different rates of the dry-down between cultivars (not shown), which was mostly explained by differences in  $E_{\text{max}}$ . The distribution of the data also showed that Semillon had a higher frequency of high rates of  $E$  than Grenache, with Syrah being intermediate (Supplementary Fig. S3). Under drought conditions,  $E$  was significantly reduced during the day for all cultivars. The highest values of  $E$  of these plants were 0.13  $\text{mmol H}_2\text{O m}^{-2} \text{s}^{-1}$  at midday without differences between cultivars. An examination of the response of  $E$  to VPD in well-watered plants ( $\psi_{\text{PD}}$  greater than  $-0.5$  MPa) revealed a linear positive relationship for the three cultivars (Fig. 2). Transpiration of

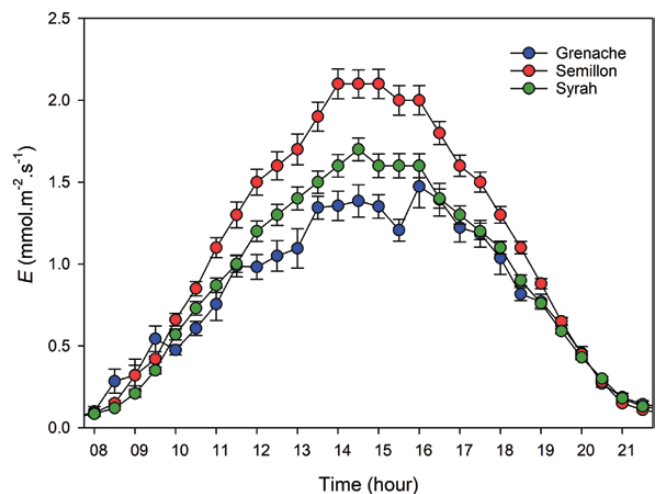


**Fig. 1.** Daytime transpiration rate measured at the whole-plant scale and expressed per leaf area in well-watered plants of Grenache, Semillon, and Syrah. Each point is the hourly mean across 15 d of the experiment  $\pm$  SE ( $n=50-60$ ).

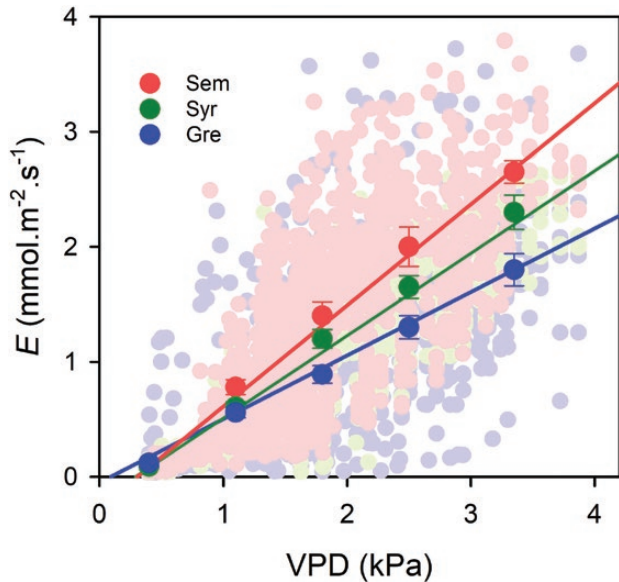


**Fig. 2.** Daytime (08.00 h–20.00 h) plant transpiration rates ( $E$ ) depending on vapor pressure deficit (VPD) in three grapevine cultivars (Grenache, Semillon, and Syrah) under well-watered conditions ( $\psi_{PD}$  greater than  $-0.5$  MPa). Significant differences were found for the slope ( $P < 0.0001$ ) of the linear regression lines (Grenache,  $E = 0.5525\text{VPD} - 0.0503$ ; Semillon,  $E = 0.8794\text{VPD} - 0.2689$ ; Syrah,  $E = 0.7171\text{VPD} - 0.2073$ ). Light colored dots are single values registered across 15 d of the experiment and dark colored dots represent the mean of  $0.5$  kPa ranges of VPD  $\pm$  SE.

the three cultivars increased with increasing VPD across a range of  $0.36$ – $3.86$  kPa; however, a clear distinction among them was observed, where Semillon and Grenache showed the highest and lowest slopes, respectively.

### Regulation of water use under water deficit

The three cultivars exhibited a sigmoidal relationship between  $G_c$  and  $\psi_{PD}$  (Fig. 3A) where  $G_c$  declines from maximum values in the range of  $\psi_{PD}$  between  $0$  and  $-0.5$  MPa to its minimum at less than  $-1.2$  MPa. Differences in the maximum level of  $G_c$  ( $G_{c\max}$ ) mirrored differences in  $E_{\max}$  (Fig. 3A, inset), with Semillon exhibiting the highest  $G_{c\max}$ , followed by Syrah and then Grenache. The sensitivity of stomata to drought varied among cultivars, with water potential at 90% of stomatal closure ( $P_{Gc90}$ , determined from  $G_c$ ) of  $-0.80$  MPa in Grenache,  $-1.00$  MPa in Syrah, and  $-1.20$  MPa in Semillon (Fig. 3A). The sensitivity of  $G_c$  to VPD (the lower the slope of the relationship  $G_c$  versus VPD the more sensitive) was greatest for Grenache and lowest for Semillon but only under well-watered conditions (Fig. 3B).

The stomatal conductance values measured with the porometer were higher (around double) than those calculated from the balances data; however, the differences between cultivars were maintained in a similar way as in Fig. 1 (not shown). Also, the water potential at 90% of stomatal closure ( $P_{g90}$ , determined from leaf-level  $g_s$ ) calculated with the porometer did not differ significantly as compared with that from the balances (Grenache =  $-0.78$  MPa, Semillon =  $-1.35$ , and Syrah =  $1.32$  MPa).

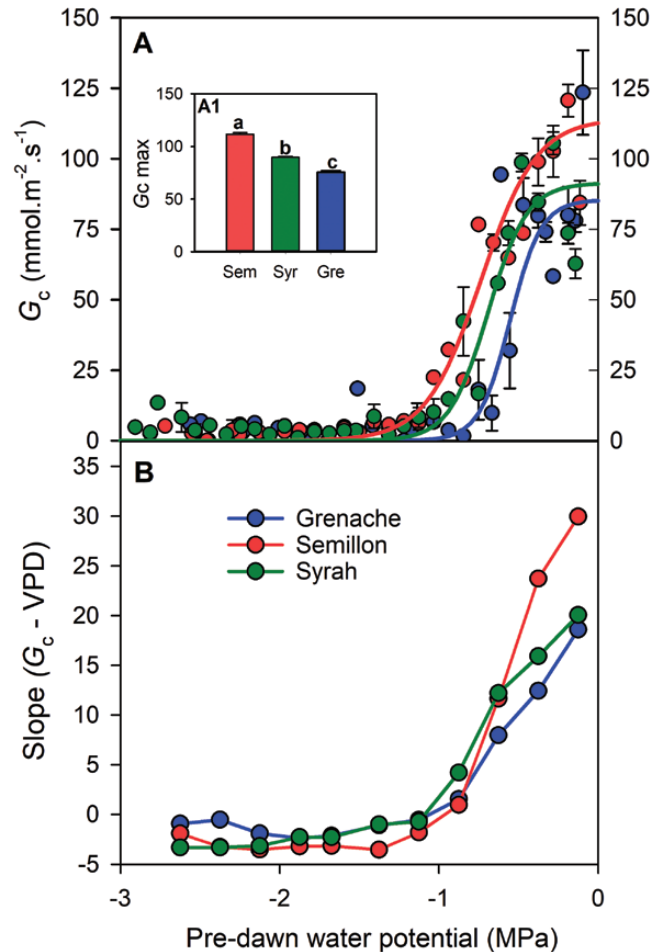


**Fig. 3.** (A) Stomatal conductance ( $G_c$ ) at the whole-plant scale (expressed per leaf area) measured between  $10.30$  h and  $15.00$  h, and (B) the slope of  $G_c$  versus VPD [Slope ( $G_c$ -VPD)] as a function of pre-dawn water potential ( $\psi_{PD}$ ) in three grapevine cultivars (Grenache, Semillon, and Syrah). Inset figure (A1), mean stomatal conductance registered between  $10.30$  h and  $15.00$  h across 15 d of the experiment under well-watered conditions ( $\psi_{PD}$  greater than  $-0.5$  MPa). In (A), each point represents the mean  $\pm$  SE of  $0.1$  MPa classes. Lines represent the best fit using sigmoid functions for each cultivar.

### Leaf hydraulic traits

Different parameters were compared between cultivars from the analysis of p–v curves (Table 1; Supplementary Fig. S1). Only  $\pi_{TLP}$  and  $\pi_0$  differed between cultivars, where Semillon showed a significantly more negative  $\pi_{TLP}$  ( $-1.92$  MPa) and  $\pi_0$  ( $-1.55$  MPa) than those of Syrah and Grenache.

The leaf minimum conductance was not different between cultivars, with presented mean values of  $\sim 9.5$   $\text{mmol m}^{-2} \text{s}^{-1}$  (Supplementary Fig. S4).

Using the optical technique (Brodribb *et al.*, 2016), leaf vulnerability to embolism was quantified in intact plants (Fig. 4). The water potential at which 12% of embolisms occurred ( $P_{12}$ ) indicated considerable variation among cultivars. Values of  $P_{12}$  were estimated at  $-1.26$  MPa for Grenache,  $-1.41$  MPa for Syrah, and  $-1.94$  MPa for Semillon. The leaf vulnerability curves constructed from the data obtained followed a sigmoidal function for all genotypes and showed variability between individual leaves, mainly for Semillon (Fig. 4A). The

**Table 1.** Pressure–volume (p–v) parameters derived from p–v analysis curves in three grapevine genotypes

Genotype	SWC	$\pi_o$ (MPa)	$\pi_{TLP}$ (MPa)	RWC <sub>TLP</sub> (%)	$\epsilon$ (MPa)	C <sub>FT</sub> (MPa <sup>-1</sup> )	C <sub>TLP</sub> (MPa <sup>-1</sup> )
Grenache	2.63±0.23	-1.18±0.07 b	-1.38±0.06 b	89.41±2.32	12.97±2.45	0.07±0.01	0.33±0.07
Semillon	2.32±0.06	-1.55±0.03 a	-1.92±0.10 a	84.58±1.80	11.8±1.49	0.08±0.01	0.32±0.06
Syrah	2.18±0.09	-1.34±0.03 b	-1.50±0.04 b	89.44±1.59	14.16±1.54	0.07±0.01	0.42±0.16
	ns	*	*	ns	ns	ns	ns

Values are the average ±SE ( $n=4$ ). Significance: \* and ns indicate significance at  $P\leq 0.05$  and not significant, respectively.

Means within columns followed by different letters differ significantly at  $P\leq 0.05$  by Fisher's multiple range test.

SWC, saturated water content;  $\pi_o$ , osmotic potential at full turgor;  $\pi_{TLP}$ , turgor loss point; RWC<sub>TLP</sub>, relative water content at turgor loss point;  $\epsilon$ , modulus of elasticity; C<sub>FT</sub>, capacitance at full turgor. C<sub>TLP</sub>, capacitance at turgor loss point.

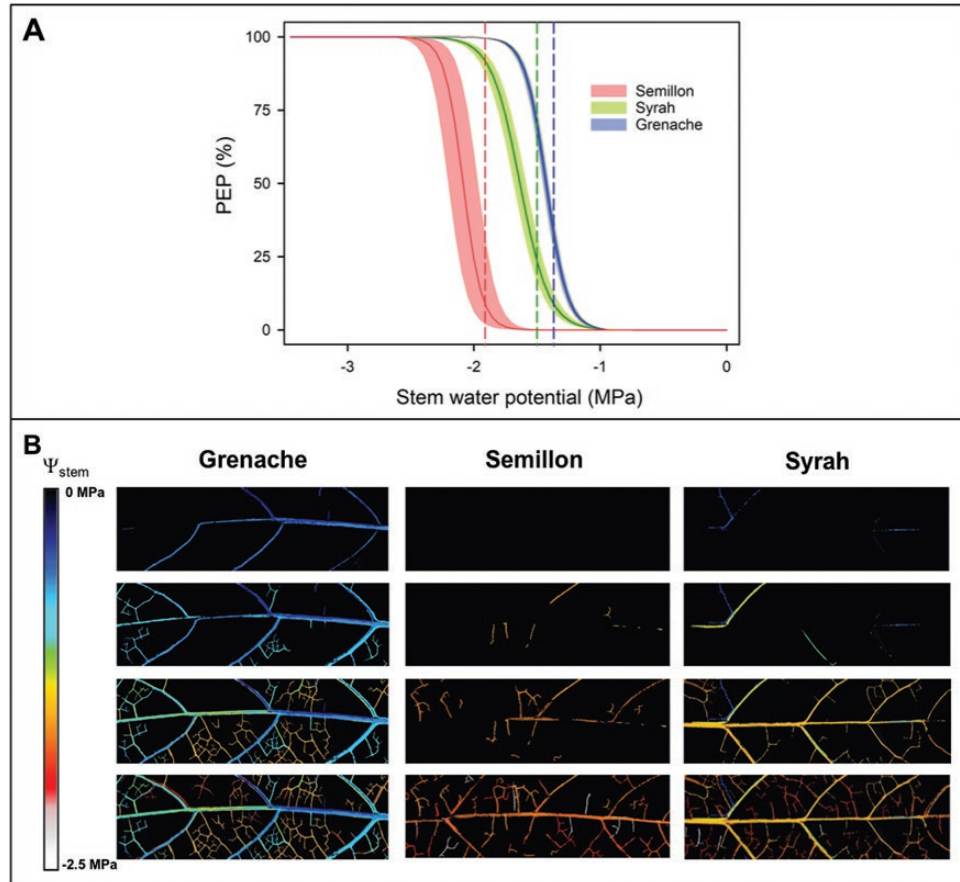


**Fig. 4.** (A) Optical vulnerability curves expressed as the percentage of embolized pixels (PEP) as a function of stem water potential in three grapevine cultivars (Grenache, Semillon, and Syrah). The solid dark line and shaded bands represent the mean observed embolism ±SE for each cultivar. The Pammenter model was first fitted per sample ( $n=4$ ) per cultivar before calculating the mean  $P_{50}$  and slope. The colored dotted lines indicate the leaf turgor loss point ( $\pi_{TLP}$ ) for each cultivar (B) Representation of leaf embolism spread during the progress of dehydration in three grapevine cultivars (Grenache, Semillon, and Syrah). Embolisms are colored according to the water potential at which they occurred (color scale shown).

water potentials at which embolism occurred was also significantly different between cultivars, where Grenache showed embolism earlier ( $P_{50}$  at -1.43 MPa), followed by Syrah ( $P_{50}$  at -1.65 MPa) and Semillon ( $P_{50}$  at -2.08 MPa). Finally, the water potentials at which 88% of the embolism occurred ( $P_{88}$ ) were observed at -1.8 MPa for Grenache, -2.24 MPa for Semillon, and -1.86 MPa for Syrah.

#### The hydraulic safety margin and trait relationships

The difference between  $P_{Gc90}$  and  $P_{12}$  were greatest for Semillon (0.74 MPa), intermediate for Grenache (0.46 MPa),

and lowest for Syrah (0.41 MPa; Fig. 5). Similarly, differences between  $P_{Gc90}$  and  $P_{50}$  (HSM  $P_{50}$ ) were greater in Semillon (0.88 MPa) followed by Syrah (0.65 MPa), and finally Grenache (0.63 MPa).

Many of the hydraulic traits quantified in the current study were well correlated with each other across the three cultivars (Supplementary Fig. S5). A cultivar's  $E_{max}$  under well-watered conditions was strongly correlated with several traits including  $P_{Gc90}$ ,  $\pi_o$ ,  $\pi_{TLP}$ , and  $P_{50}$  (Fig. 6). A cultivar's  $P_{50}$  was strongly correlated with  $P_{Gc90}$ ,  $\pi_o$ ,  $\pi_{TLP}$ , C<sub>FT</sub>, and RWC<sub>TLP</sub> (Supplementary Fig. S5). Finally, a cultivar's HSM  $P_{50}$  was strongly correlated with several traits, including  $\pi_{TLP}$ .

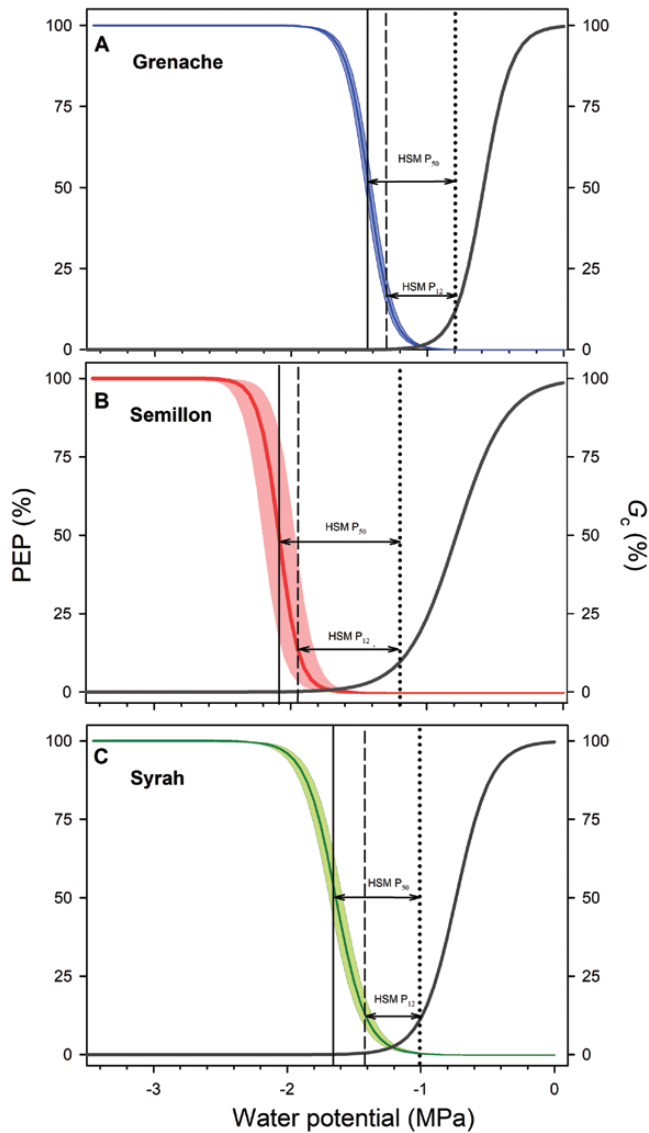


**Fig. 5.** Optical hydraulic vulnerability curves (PEP %) and stomatal conductance ( $G_c$  %) as a response of the organ (stem for PEP % and leaf for  $G_c$ ) water potential in three grapevine cultivars, (A) Grenache, (B) Semillon, and (C) Syrah. The  $P_{Gc90}$ ,  $P_{50}$ , and  $P_{88}$  are indicated by a dotted, dashed, and solid black line, respectively. The hydraulic safety margins at  $P_{50}$  (HSM  $P_{50}$ ) and at  $P_{12}$  (HSM  $P_{12}$ ) are indicated by arrows.

### Simulating the time of survival under drought

Drought simulations performed with the Sur\_Eau model using the hydraulic traits empirically determined in this study showed that when the three different cultivars are placed under identical environmental conditions, the maximum water use ( $E_{plant}$ ) decreased earlier or later depending on the cultivar. For instance,  $E_{plant}$  decreased significantly after 1.5 d in Semillon, 2.0 d in Syrah, and 2.5 d in Grenache (Fig. 7). Also, the predicted time in this ‘generic scenario’ needed to reach  $P_{50}$  (used here to approximate mortality) was also different across cultivars where Semillon reached  $P_{50}$  in 3.5 d, Syrah in 3.75 d, and Grenache in 4.2 d. When including variable climatic conditions (day/night simulations) in the model, the predicted time needed to reach  $P_{50}$  was higher for all the cultivars, being 7.3 d in Semillon, 7.6 d in Syrah, and 8.7 d in Grenache (Supplementary Fig. S6).

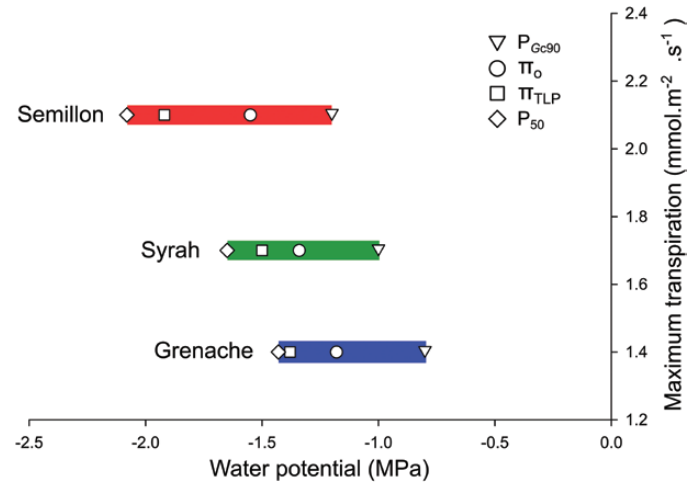


**Fig. 6.** Relationships between the maximum transpiration rate for the three cultivars under well-watered conditions and the leaf-level hydraulic traits  $P_{Gc90}$ ,  $\pi_0$ ,  $\pi_{TLP}$ , and  $P_{50}$ . Bars correspond to the HSM  $P_{50}$ . Pearson correlations between all parameters can be found in Supplementary Fig. S5.

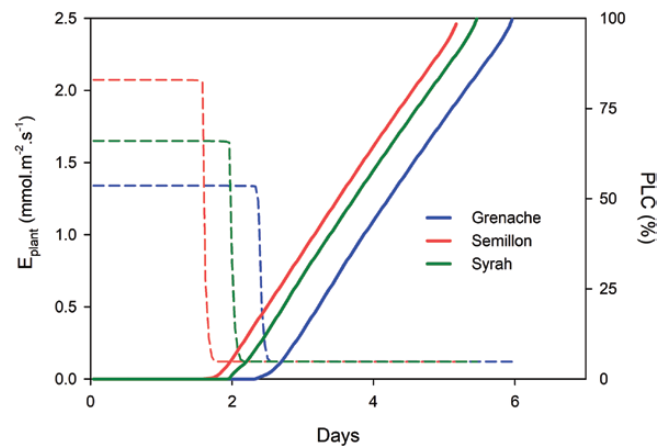


**Fig. 7.** Simulated declining of maximum water use ( $E_{plant}$ ; dotted lines) and increasing loss of hydraulic conductivity (PLC%; solid lines) over time (days) under identical environmental conditions during the progression of drought in three grapevine cultivars (Grenache, Semillon, and Syrah) using the Sur\_Eau model (Martin-StPaul et al., 2017).

## Discussion

In this study, we integrated hydraulic traits to explain the drought responses of three contrasting grapevine varieties across a wide range of soil water deficit and VPD conditions. Cultivars differed in multiple traits examined, including  $E_{max}$ , stomatal regulation,  $\pi_{TLP}$ ,  $\pi_0$ , and leaf vulnerability to embolism ( $P_{50}$ ). Despite these differences, all cultivars closed their stomata prior to leaf embolism formation. The maximum water use given by  $E_{max}$  was strongly correlated with other drought traits (e.g.  $P_{Gc90}$ ,  $\pi_{TLP}$ , and leaf  $P_{50}$ ) and thus the higher  $E$  in Semillon corresponded to a less vulnerable leaf exhibiting a more negative  $\pi_{TLP}$  and leaf  $P_{50}$ . There was substantial variation of the cultivars’ HSMs, and model simulations suggest that despite Grenache’s narrower HSM, its more conservative water use results in it having a longer time to hydraulic failure than the other cultivars.

### Maximum transpiration

Monitoring real-time whole-plant water use in the minilysimeter phenotyping platform revealed differences in the water use behavior between the three cultivars. Under well-watered conditions, Semillon had greater water use over a wide range of VPD conditions (Figs 1, 2). It has been reported that Semillon displays higher rates of daytime (and night-time) transpiration under field conditions when compared with other grapevine cultivars (Rogiers et al., 2009). Under well-watered conditions and saturating values of radiation (PPDF >800  $\mu\text{mol m}^{-2} \text{s}^{-1}$ ),  $E$  responded linearly to VPD in all genotypes since VPD is a main driver of transpiration (Oren et al., 1999; Schultz and Stoll, 2010; Rogiers et al., 2011; Devi and Reddy, 2018). A linear relationship between  $E$  and VPD was also observed across a diverse set of species under well-watered conditions (Oren et al., 1999). Semillon also exhibited a low sensitivity of  $G_c$  to VPD under well-watered conditions. Grapevine  $G_c$  has been shown to be relatively insensitive to VPD under well-watered conditions (Rogiers et al., 2011; Charrier et al., 2018), and grapevines have been shown to maintain high levels of  $E$  and  $G_c$  even at very high temperatures (>40 °C) when supplied with ample irrigation (Greer, 2012).

### Stomatal regulation

A decline of stomatal conductance was observed with increasing soil water deficit in all cultivars (Fig. 3A). However, Grenache exhibited a more rapid decline and a higher sensitivity of  $G_c$  to increasing VPD. These results are consistent with previous studies that suggest that Grenache regulates  $\psi_{\text{leaf}}$  more ‘conservatively’ than other varieties, exhibiting an isohydric behavior (Schultz, 2003). However, differences in the stomatal sensitivity to VPD between cultivars occurred only within a narrow range of pre-dawn water potentials (greater than  $-1$  MPa), below which all cultivars displayed a similar response (Fig. 3B). Recent investigations on different grapevine cultivars and rootstocks also observed that differences between cultivars in the regulation of  $G_c$  were only present under well-watered and mild stress conditions (greater than  $-0.8$  MPa) (Peccoux et al., 2017; Charrier et al., 2018). The complexity of the relationships between stomatal regulation, soil water potential, and VPD makes assigning distinct water use behaviors (e.g. iso/anisohydric) difficult (Hochberg et al., 2018) and so we sought to integrate these behaviors with other hydraulic traits.

In this study,  $G_c$  was calculated from whole-plant transpiration using Equation 2 which uses ambient VPD as the driving force for the calculation. This allows for the use of a much greater amount of data recorded in real time by the minilysimeter platform, which is critical for larger scale phenotyping and more robust statistical analysis. However, the use of ambient temperature and not leaf temperature could bias our results, and studies have shown that in complex grapevine canopies, the degree of coupling between the canopy and atmosphere can be complex (Buckley et al., 2014). Therefore, we also carried out leaf-level stomatal conductance measurements which were strongly correlated with values of  $G_c$  ( $r^2=0.79$ ,  $P<0.0001$ ,

data not shown), and our values of  $P_{g90}$  calculated from leaf-level measurements did not differ significantly from  $P_{Gc90}$ . Additionally, previous studies from our laboratory have shown a strong correlation between stomatal conductance measurements made at the leaf- and whole-plant levels (Charrier et al., 2018) in our experimental context. Future studies could aim at using more robust methods of extrapolating stomatal conductance from whole-plant water use data.

### Leaf-level hydraulic traits

In our study, the more negative  $P_{Gc90}$  values observed in Syrah and Semillon could allow them to operate over a wider range of water potentials, and this is likely to be due in part to their lower osmotic potential at full hydration ( $\pi_0$ ) and leaf turgor loss ( $\pi_{\text{TLP}}$ ) relative to Grenache (Table 1). It has been suggested that the  $\pi_{\text{TLP}}$  is related to a plant’s ability to ‘tolerate’ drought rather than to avoid it by closing the stomata or shedding leaves (Brodribb and Holbrook, 2003). Other p-v parameters have also been proposed as strong predictors of drought tolerance, such as the modulus of elasticity (Niinemets, 2001; Brodribb and Holbrook, 2003; Read et al., 2006). An interesting meta-analysis conducted across many species concluded that  $\pi_{\text{TLP}}$  showed a strong association with water availability within and across habitats and that  $\pi_0$  and  $\pi_{\text{TLP}}$  were the only two parameters that clearly delimited species associated with wet and dry habitats (Bartlett et al., 2012). The same study showed that variations in  $\pi_{\text{TLP}}$  among and within species were mainly driven by osmotic ( $\pi_0$ ) rather than elastic adjustments to maintain  $\text{RWC}_{\text{TLP}}$  and prevent cell dehydration. In our study, Semillon also showed a significantly lower  $\pi_0$  than Syrah and Grenache, suggesting that osmotic adjustment was the main driver of its more negative turgor loss point. The ability to generate solutes or tolerate an increased symplastic solute concentration has been observed to differ between species (Zhang et al., 1999). Because producing solutes generates a metabolic cost, some species will rely (or are more plastic) on other physiological traits to survive drought such as root morphology, water use efficiency, and xylem cavitation resistance (Vandeleur et al., 2009; Choat et al., 2010; Bartlett et al., 2012; Gambetta et al., 2013; Barrios-Macias et al., 2015). Based on these observations, it is reasonable to conclude that the ability of Semillon to maintain cell turgor at a lower  $\psi_{\text{leaf}}$  allowed this cultivar to operate across a wider range of soil water deficit and VPD conditions than Syrah and Grenache.

### Leaf vulnerability to embolism

Leaves of the different cultivars varied significantly in their vulnerability to embolism (Fig. 4). Only a few studies to date (e.g. Martorell et al., 2015) have compared the leaf hydraulic vulnerability between different grapevine genotypes in the same study. The range of leaf  $P_{50}$  values (ranging from  $-1.4$  MPa to  $-2$  MPa) in the current study was consistent with the leaf  $P_{50}$  values in Syrah ( $-1.5$  MPa; Hochberg et al., 2016) and Chardonnay ( $-1.5$  MPa to  $-2.0$  MPa; Hochberg, 2017b). Interestingly, all cultivars experienced enough stomatal closure before any leaf embolisms were observed (Fig. 5). Our results



argue against the hypothesis that the induction of embolism could act as a signal for stomatal closure (Nardini and Salleo, 2000) and support the recent findings that significant embolism occurs after stomatal closure under prolonged drought conditions (Hochberg *et al.*, 2016; Martin-StPaul *et al.*, 2017; Creek *et al.*, 2020).

In the current study stomatal regulation is related to pre-dawn water potentials (Fig. 3A) while vulnerability is related to stem water potentials (Fig. 4A). It would have been more appropriate to use the stem water potentials at the time of stomatal conductance since there is a possibility that, relative to the vulnerability thresholds,  $P_{Gc90}$  would be slightly overestimated, making the resulting HSM overestimated as well. However, this is unlikely since at  $P_{Gc90}$ , pre-dawn and midday water potentials collapse to the same value (i.e.  $\psi_{PD} \sim \psi_{Stem}$ ) which has been shown before for two of the same cultivars (Grenache and Syrah) within the same experimental system (Charrier *et al.*, 2018).

#### Linking traits: from $E_{max}$ to stomatal closure, to leaf vulnerability

In our study  $E_{max}$  under well-watered conditions was strongly correlated with numerous leaf-level hydraulic traits including  $P_{Gc90}$ ,  $\pi_0$ ,  $\pi_{TLP}$ , and  $P_{50}$  (Fig. 6). This suggests that as maximum water use increases, leaf hydraulic traits are well integrated, preparing the leaf to operate across a wider range of water potentials. Simonin *et al.* (2014) demonstrated that across several forest tree species, leaf hydraulic conductance increases with increasing  $E$ . In that study, although the increase in leaf hydraulic conductance buffered variation in  $\psi_{leaf}$ , increasing  $E$  led to more negative  $\psi_{leaf}$  increasing the range of  $\psi_{leaf}$  experienced by the plants. Similarly, a close relationship between leaf turgor loss, loss of hydraulic conductance, and stomatal closure was observed in different tree species, suggesting that stomatal closure is coordinated with leaf hydraulic conductance (Brodrribb and Holbrook, 2003). In the current study, other leaf-level hydraulic traits were also well coordinated with each other (Supplementary Fig. S5), consistent with previous studies (Bartlett *et al.*, 2016). This raises the possibility that leaf hydraulic traits are largely interdependent and raises questions about the extent to which these traits can be disentangled (Reich, 2014).

Complete stomatal closure occurred prior to the  $\pi_{TLP}$  for all cultivars, indicating that the stomatal response to  $\psi_{leaf}$  occurs as mesophyll cell turgor declines (Fig. 5; Table 1). Similar results have been found previously for the grapevine cultivar Merlot (Hochberg *et al.*, 2017a). A recent study in a number of species of different biomes indicated that the water potential causing stomatal closure is closely related to  $\pi_{TLP}$  in most of the species (Martin-StPaul *et al.*, 2017). However, studies across other species have shown that the relationship between stomatal closure and  $\pi_{TLP}$  can vary, with some species closing stomata coincident with, and others prior to, the  $\pi_{TLP}$  (e.g. Brodrribb and Holbrook, 2003; Guyot *et al.*, 2012). Such uncoupling between stomatal closure and  $\pi_{TLP}$  is supported by previous evidence showing that guard cells can act independently from the rest of the leaf (Mott and Franks, 2001). Stomatal closure prior to

$\pi_{TLP}$  is considered a drought tolerance mechanism enabling a plant to survive on stored water (which would be slowly lost considering a low minimal conductance) after stomatal closure (Guyot *et al.*, 2012; Delzon, 2015; Duursma *et al.*, 2019).

A cultivar's  $\pi_{TLP}$  was closely related to the onset of leaf xylem embolism (Fig. 4). Although we did not quantify leaf mortality in the current study we carried out a re-analysis with the results obtained by Charrier *et al.* (2018) in order to examine the relationship between leaf PLC and mortality for Grenache and Syrah. In both cultivars, water potential values corresponding to high levels of leaf PLC (>50%, or even 88%) in the current study corresponded to low levels of leaf mortality in the study of Charrier *et al.* (2018), from 5% to 10% in Grenache and from 20% to 30% in Syrah. This supports the hypothesis that significant levels of leaf embolism precede leaf mortality in grapevine (Hochberg *et al.*, 2016) and other angiosperms (Urli *et al.*, 2013; Choat *et al.*, 2018).

Because the HSM can be used to predict tree mortality rates in many forest biomes, it has been used to evaluate the degree of conservatism in plant hydraulic strategies to drought (Brodrribb *et al.*, 2010; McDowell *et al.*, 2011; Choat *et al.*, 2013). In our study, the cultivar that had the most negative  $P_{50}$  (Semillon) also exhibited the largest HSM when compared with the other cultivars (Fig. 5). Despite this, there appears to be no systematic relationship between  $P_{50}$  and the size of the HSM. Grenache, for example, with the least negative  $P_{50}$  still maintained a significant HSM because of its less negative  $P_{gs90}$ . The results of the simulations performed with the model Sur\_Eau showed that the most 'conservative' cultivar (Grenache) could be considered the most drought tolerant because the time needed to reach  $P_{50}$  is greater than for the other cultivars (Fig. 7; Supplementary Fig. S6). This is intriguing given that Grenache is widely considered a drought-tolerant cultivar that is selectively chosen for cultivation in hot, dry wine regions. This result also illustrates that the timing of hydraulic failure does not correlate directly with the size of the HSM and instead is a more complex process where other traits such as stomatal regulation and minimal conductance are involved.

Differences in the size of the leaf HSM between cultivars could be brought about by differences in  $P_{Gc90}$  and/or leaf  $P_{50}$ . In the current study,  $P_{Gc90}$  and  $P_{50}$  (and  $\pi_{TLP}$ ) were well correlated with each other, and with  $E_{max}$  (discussed above), with greater  $E_{max}$  corresponding to a more negative  $P_{Gc90}$ ,  $\pi_{TLP}$ , and  $P_{50}$  (Fig. 6). Recent investigations demonstrated that across diverse species,  $\pi_{TLP}$  was positively correlated with leaf minimum water potential and vulnerability to embolism (i.e. the less negative the  $\pi_{TLP}$ , the greater the HSM), although the variation within this relationship was extremely large (Zhu *et al.*, 2018). This correlation does not hold between the grapevine cultivars examined here. For example, Semillon exhibited the most negative  $P_{50}$  and  $\pi_{TLP}$ , and the largest safety margin (Figs 4, 5). These results support the idea that although water use and leaf hydraulic traits are often correlated, these relationships are variable even within a single species such as grapevine (Brodrribb *et al.*, 2003; Choat *et al.*, 2018).

The exact mechanisms leading to correlations between traits and observed differences in the HSM remain

unknown. Once the stomata close, the plant relies on the internal stored water for survival (Blackman *et al.*, 2016), and its depletion after stomatal closure depends mostly on the minimum conductance,  $g_{\min}$  (Duursma *et al.*, 2019). This is the first study to quantify  $g_{\min}$  in grapevine, and we did not find differences in  $g_{\min}$  between the three cultivars (Supplementary Fig. S4), with the absolute values being similar to those of several other crop species (Duursma *et al.*, 2019). Other traits that could potentially influence the HSM could include leaf capacitance, leaf shrinkage (Scoffoni *et al.*, 2014), transpiration area variation (i.e. leaf shedding), and total leaf water storage (Choat *et al.*, 2018). Processes that occur after leaf stomatal closure are surely critical and deserve more attention.

### Conclusions

This is among one of a few studies on grapevine that has attempted to integrate multiple drought behavior traits. All cultivars closed stomata prior to reaching water potential values that would cause leaf hydraulic failure. Traits that allow a cultivar to tolerate lower  $\psi_{\text{leaf}}$ , such as  $\pi_0$ ,  $\pi_{\text{TLP}}$ , and  $P_{50}$ , were tightly correlated with a cultivar's maximum water use under well-watered conditions. Despite these correlations, there was substantial variability in the HSM between cultivars, suggesting that the relationships between leaf hydraulic traits are labile even within a single species such as grapevine. The results of this study demonstrate that the relationships between traits such as stomatal regulation, leaf embolism thresholds, and survival time under drought are complex and interactive, stressing the importance of integrating multiple physiological traits in characterizing drought tolerance.

### Supplementary data

Supplementary data are available at *JXB* online.

Fig. S1. Pressure–volume curves plotted as  $-1/\psi$  versus RWC for each cultivar.

Fig. S2. Correlation between pre-dawn water potential and soil relative water content.

Fig. S3. Variability of diurnal plant transpiration. (A) Boxplot and (B) histogram.

Fig. S4. Minimum leaf conductance for each cultivar.

Fig. S5. Pearson correlations between the measured hydraulic traits.

Fig. S6. Simulation with the Sur\_Eau model under variable climatic conditions.

### Acknowledgements

This work was supported by the EU, ERA-NET, ARIMNET2 project, Opportunities for an Environmental-friendly Viticulture: EnViRoS. This work was also supported by the 'Investments for the Future' (ANR-10-EQPX-16, XYLOFOREST) program and the Cluster of Excellence COTE (ANR-10-LABX-45) of the French National Agency for Research. This work is also conducted as part of the LIA INNOGRAPE International Associated Laboratory.

### References

- Anderegg WR, Klein T, Bartlett M, Sack L, Pellegrini AF, Choat B, Jansen S. 2016. Meta-analysis reveals that hydraulic traits explain cross-species patterns of drought-induced tree mortality across the globe. *Proceedings of the National Academy of Sciences, USA* **113**, 5024–5029.
- Anderegg WRL, Meinzer FC. 2015. Wood anatomy and plant hydraulics in a changing climate. In: Hacke U, ed. *Functional and ecological xylem anatomy*. Cham: Springer International Publishing, 235–253.
- Barrios-Masias FH, Knipfer T, McElrone AJ. 2015. Differential responses of grapevine rootstocks to water stress are associated with adjustments in fine root hydraulic physiology and suberization. *Journal of Experimental Botany* **66**, 6069–6078.
- Bartlett MK, Klein T, Jansen S, Choat B, Sack L. 2016. The correlations and sequence of plant stomatal, hydraulic, and wilting responses to drought. *Proceedings of the National Academy of Sciences, USA* **113**, 13098–13103.
- Bartlett MK, Scoffoni C, Sack L. 2012. The determinants of leaf turgor loss point and prediction of drought tolerance of species and biomes: a global meta-analysis. *Ecology Letters* **15**, 393–405.
- Blackman CJ, Pfautsch S, Choat B, Delzon S, Gleason SM, Duursma RA. 2016. Toward an index of desiccation time to tree mortality under drought. *Plant, Cell & Environment* **39**, 2342–2345.
- Brodribb TJ, Bowman DJ, Nichols S, Delzon S, Burtlett R. 2010. Xylem function and growth rate interact to determine recovery rates after exposure to extreme water deficit. *New Phytologist* **188**, 533–542.
- Brodribb TJ, Holbrook NM. 2003. Stomatal closure during leaf dehydration, correlation with other leaf physiological traits. *Plant Physiology* **132**, 2166–2173.
- Brodribb TJ, Holbrook NM, Edwards EJ, Gutiérrez MV. 2003. Relations between stomatal closure, leaf turgor and xylem vulnerability in eight tropical dry forest trees. *Plant, Cell & Environment* **26**, 443–450.
- Brodribb TJ, Skelton RP, McAdam SA, Bienaimé D, Lucani CJ, Marmottant P. 2016. Visual quantification of embolism reveals leaf vulnerability to hydraulic failure. *New Phytologist* **209**, 1403–1409.
- Buckley TN, Martorell S, Diaz-Espejo A, Tomàs M, Medrano H. 2014. Is stomatal conductance optimized over both time and space in plant crowns? A field test in grapevine (*Vitis vinifera*). *Plant, Cell & Environment* **37**, 2707–2721.
- Campbell GS. 1974. A simple method for determining unsaturated conductivity from moisture retention data. *Soil science* **117**, 311–314.
- Cattivelli L, Rizza F, Badeck FW, Mazzucotelli E, Mastrangelo AM, Francia E, Marè C, Tondelli A, Stanca AM. 2008. Drought tolerance improvement in crop plants: an integrated view from breeding to genomics. *Field Crops Research* **105**, 1–4.
- Charrier G, Delzon S, Domec JC, *et al.* 2018. Drought will not leave your glass empty: low risk of hydraulic failure revealed by long-term drought observations in world's top wine regions. *Science Advances* **4**, eaao6969.
- Chaves MM, Zarrouk O, Francisco R, Costa JM, Santos T, Regalado AP, Rodrigues ML, Lopes CM. 2010. Grapevine under deficit irrigation: hints from physiological and molecular data. *Annals of Botany* **105**, 661–676.
- Choat B. 2013. Predicting thresholds of drought-induced mortality in woody plant species. *Tree Physiology* **33**, 669–671.
- Choat B, Brodribb TJ, Brodersen CR, Duursma RA, López R, Medlyn BE. 2018. Triggers of tree mortality under drought. *Nature* **558**, 531–539.
- Choat B, Drayton WM, Brodersen C, Matthews MA, Shackel KA, Wada H, McElrone AJ. 2010. Measurement of vulnerability to water stress-induced cavitation in grapevine: a comparison of four techniques applied to a long-veined species. *Plant, Cell & Environment* **33**, 1502–1512.
- CoupeL-Ledru A, Lebon E, Christophe A, Gallo A, Gago P, Pantin F, Doligez A, Simonneau T. 2016. Reduced nighttime transpiration is a relevant breeding target for high water-use efficiency in grapevine. *Proceedings of the National Academy of Sciences, USA* **113**, 8963–8968.
- CoupeL-Ledru A, Tyerman SD, Masclef D, Lebon E, Christophe A, Edwards EJ, Simonneau T. 2017. Abscisic acid down-regulates hydraulic conductance of grapevine leaves in isohydric genotypes only. *Plant Physiology* **175**, 1121–1134.

- Creek D, Lamarque LJ, Torres-Ruiz JM, Parise C, Burlett R, Tissue DT, Delzon S.** 2020. Xylem embolism in leaves does not occur with open stomata: evidence from direct observations using the optical visualization technique. *Journal of Experimental Botany* **71**, 1151–1159.
- Delzon S.** 2015. New insight into leaf drought tolerance. *Functional Ecology* **29**, 1247–1249.
- Delzon S, Cochard H.** 2014. Recent advances in tree hydraulics highlight the ecological significance of the hydraulic safety margin. *New Phytologist* **203**, 355–358.
- Devi MJ, Reddy VR.** 2018. Transpiration response of cotton to vapor pressure deficit and its relationship with stomatal traits. *Frontiers in Plant Science* **9**, 1572.
- Duursma RA, Blackman CJ, Lopéz R, Martin-StPaul NK, Cochard H, Medlyn BE.** 2019. On the minimum leaf conductance: its role in models of plant water use, and ecological and environmental controls. *New Phytologist* **221**, 693–705.
- Ewers BE, Oren R, Phillips N, Strömberg M, Linder S.** 2001. Mean canopy stomatal conductance responses to water and nutrient availabilities in *Picea abies* and *Pinus taeda*. *Tree Physiology* **21**, 841–850.
- Gambetta GA, Fei J, Rost TL, Knipfer T, Matthews MA, Shackel KA, Walker MA, McElrone AJ.** 2013. Water uptake along the length of grapevine fine roots: developmental anatomy, tissue-specific aquaporin expression, and pathways of water transport. *Plant Physiology* **163**, 1254–1265.
- Gerzon E, Biton I, Yaniv Y, Zemach H, Netzer Y, Schwartz A, Fait A, Ben-Ari G.** 2015. Grapevine anatomy as a possible determinant of isohydric or anisohydric behavior. *American Journal of Enology and Viticulture* **66**, 340–347.
- Greer DH.** 2012. Modelling leaf photosynthetic and transpiration temperature-dependent responses in *Vitis vinifera* cv. Semillon grapevines growing in hot, irrigated vineyard conditions. *AoB Plants* **2012**, pls009.
- Guyot G, Scoffoni C, Sack L.** 2012. Combined impacts of irradiance and dehydration on leaf hydraulic conductance: insights into vulnerability and stomatal control. *Plant, Cell & Environment* **35**, 857–871.
- Hammond WM, Yu K, Wilson LA, Will RE, Anderegg WRL, Adams HD.** 2019. Dead or dying? Quantifying the point of no return from hydraulic failure in drought-induced tree mortality. *New Phytologist* **223**, 1834–1843.
- Hochberg U, Albuquerque C, Rachmilevitch S, Cochard H, David-Schwartz R, Brodersen CR, McElrone A, Windt CW.** 2016. Grapevine petioles are more sensitive to drought induced embolism than stems: evidence from in vivo MRI and microcomputed tomography observations of hydraulic vulnerability segmentation. *Plant, Cell & Environment* **39**, 1886–1894.
- Hochberg U, Bonel AG, David-Schwartz R, Degu A, Fait A, Cochard H, Peterlunger E, Herrera JC.** 2017a. Grapevine acclimation to water deficit: the adjustment of stomatal and hydraulic conductance differs from petiole embolism vulnerability. *Planta* **245**, 1091–1104.
- Hochberg U, Herrera JC, Cochard H, Badel E.** 2016. Short-time xylem relaxation results in reliable quantification of embolism in grapevine petioles and sheds new light on their hydraulic strategy. *Tree Physiology* **36**, 748–755.
- Hochberg U, Rockwell FE, Holbrook NM, Cochard H.** 2018. Iso/anisohydry: a plant–environment interaction rather than a simple hydraulic trait. *Trends in Plant Science* **23**, 112–120.
- Hochberg U, Windt CW, Ponomarenko A, Zhang YJ, Gersony J, Rockwell FE, Holbrook NM.** 2017b. Stomatal closure, basal leaf embolism, and shedding protect the hydraulic integrity of grape stems. *Plant Physiology* **174**, 764–775.
- Hopper DW, Ghan R, Cramer GR.** 2014. A rapid dehydration leaf assay reveals stomatal response differences in grapevine genotypes. *Horticulture Research* **22**, 1–2.
- Martin-StPaul N, Delzon S, Cochard H.** 2017. Plant resistance to drought depends on timely stomatal closure. *Ecology Letters* **20**, 1437–1447.
- Martorell S, Medrano H, Tomàs M, Escalona JM, Flexas J, Diaz-Espejo A.** 2015. Plasticity of vulnerability to leaf hydraulic dysfunction during acclimation to drought in grapevines: an osmotic-mediated process. *Physiologia Plantarum* **153**, 381–391.
- McDowell NG.** 2011. Mechanisms linking drought, hydraulics, carbon metabolism, and vegetation mortality. *Plant Physiology* **155**, 1051–1059.
- Meinzer FC, Johnson DM, Lachenbruch B, McCulloh KA, Woodruff DR.** 2009. Xylem hydraulic safety margins in woody plants: coordination of stomatal control of xylem tension with hydraulic capacitance. *Functional Ecology* **23**, 922–930.
- Monteith JL, Unsworth MH.** 1990. Principles of environmental physics. London: Edward Arnold.
- Mott KA, Franks PJ.** 2001. The role of epidermal turgor in stomatal interactions following a local perturbation in humidity. *Plant, Cell & Environment* **24**, 657–662.
- Nardini A, Salleo S.** 2000. Limitation of stomatal conductance by hydraulic traits: sensing or preventing xylem cavitation? *Trees* **15**, 14–24.
- Niinemets Ü.** 2001. Global-scale climatic controls of leaf dry mass per area, density, and thickness in trees and shrubs. *Ecology* **82**, 453–469.
- Oren R, Sperry JS, Katul GG, Pataki DE, Ewers BE, Phillips N, Schäfer KV.** 1999. Survey and synthesis of intra- and interspecific variation in stomatal sensitivity to vapor pressure deficit. *Plant, Cell & Environment* **22**, 1515–1526.
- Pammenter NV, Van der Willigen C.** 1998. A mathematical and statistical analysis of the curves illustrating vulnerability of xylem to cavitation. *Tree Physiology* **18**, 589–593.
- Peccoux A, Loveys B, Zhu J, Gambetta GA, Delrot S, Vivin P, Schultz HR, Ollat N, Dai Z.** 2018. Dissecting the rootstock control of scion transpiration using model-assisted analyses in grapevine. *Tree Physiology* **38**, 1026–1040.
- Phillips N, Oren R.** 1998. A comparison of daily representations of canopy conductance based on two conditional time-averaging methods and the dependence of daily conductance on environmental factors. *Annales des Sciences Forestières* **55**, 217–235.
- Pou A, Medrano H, Tomàs M, Martorell S, Ribas-Carbó M, Flexas J.** 2012. Anisohydric behaviour in grapevines results in better performance under moderate water stress and recovery than isohydric behaviour. *Plant and Soil* **359**, 335–349.
- Read J, Sanson GD, Garine-Wichatitsky Md, Jaffré T.** 2006. Sclerophylly in two contrasting tropical environments: low nutrients vs. low rainfall. *American Journal of Botany* **93**, 1601–1614.
- Reich PB.** 2014. The world-wide ‘fast–slow’ plant economics spectrum: a traits manifesto. *Journal of Ecology* **102**, 275–301.
- Rogiers SY, Greer DH, Hatfield JM, Hutton RJ, Clarke SJ, Hutchinson PA, Somers A.** 2012. Stomatal response of an anisohydric grapevine cultivar to evaporative demand, available soil moisture and abscisic acid. *Tree Physiology* **32**, 249–261.
- Rogiers SY, Greer DH, Hutton RJ, Landsberg JJ.** 2009. Does night-time transpiration contribute to anisohydric behaviour in a *Vitis vinifera* cultivar? *Journal of Experimental Botany* **60**, 3751–3763.
- Sack L, Pasquet-Kok J.** 2011. Leaf pressure–volume curve parameters. PrometheusWiki website: <http://prometheuswiki.org/wiki/index.php?page=Leaf+pressure-volume+curve+parameters>.
- Schultz HR.** 2003. Differences in hydraulic architecture account for near-isohydric and anisohydric behaviour of two field-grown *Vitis vinifera* L. cultivars during drought. *Plant, Cell & Environment* **26**, 1393–1405.
- Schultz HR, Stoll M.** 2010. Some critical issues in environmental physiology of grapevines: future challenges and current limitations. *Australian Journal of Grape and Wine Research* **16**, 4–24.
- Schuster AC, Burghardt M, Riederer M.** 2017. The ecophysiology of leaf cuticular transpiration: are cuticular water permeabilities adapted to ecological conditions? *Journal of Experimental Botany* **68**, 5271–5279.
- Scoffoni C, Vuong C, Diep S, Cochard H, Sack L.** 2014. Leaf shrinkage with dehydration: coordination with hydraulic vulnerability and drought tolerance. *Plant Physiology* **164**, 1772–1788.
- Simonin KA, Burns E, Choat B, Barbour MM, Dawson TE, Franks PJ.** 2015. Increasing leaf hydraulic conductance with transpiration rate minimizes the water potential drawdown from stem to leaf. *Journal of Experimental Botany* **66**, 1303–1315.
- Tardieu F, Simonneau T.** 1998. Variability among species of stomatal control under fluctuating soil water status and evaporative demand: modelling isohydric and anisohydric behaviours. *Journal of Experimental Botany* **49**, 419–432.
- Tyree MT, Hammel HT.** 1972. The measurement of the turgor pressure and the water relations of plants by the pressure-bomb technique. *Journal of Experimental Botany* **23**, 267–282.
- Tyree MT, Sperry JS.** 1989. Vulnerability of xylem to cavitation and embolism. *Annual Review of Plant Biology* **40**, 19–36.

**Urli M, Porté AJ, Cochard H, Guengant Y, Burlett R, Delzon S.** 2013. Xylem embolism threshold for catastrophic hydraulic failure in angiosperm trees. *Tree Physiology* **33**, 672–683.

**Vandeleur RK, Mayo G, Shelden MC, Gilliam M, Kaiser BN, Tyerman SD.** 2009. The role of plasma membrane intrinsic protein aquaporins in water transport through roots: diurnal and drought stress responses reveal different strategies between isohydric and anisohydric cultivars of grapevine. *Plant Physiology* **149**, 445–460.

**Van Genuchten MT.** 1980. A closed-form equation for predicting the hydraulic conductivity of unsaturated soils 1. *Soil Science Society of America Journal* **44**, 892–898.

**Zhang J, Nguyen HT, Blum A.** 1999. Genetic analysis of osmotic adjustment in crop plants. *Journal of Experimental Botany* **50**, 291–302.

**Zhu SD, Chen YJ, Ye Q, He PC, Liu H, Li RH, Fu PL, Jiang GF, Cao KF.** 2018. Leaf turgor loss point is correlated with drought tolerance and leaf carbon economics traits. *Tree Physiology* **38**, 658–663.